

## Electrical impedance for an electrolytic cell

F. C. M. Freire,<sup>1,2,\*</sup> G. Barbero,<sup>1,3,†</sup> and M. Scalerandi<sup>1,‡</sup>

<sup>1</sup>*Dipartimento di Fisica, Politecnico di Torino, Corso Duca degli Abruzzi, 24, 10129 Torino, Italy*

<sup>2</sup>*Departamento de Física, Universidade Estadual de Maringá, Av. Colombo 5790, 87020-900 Maringá, PR, Brazil*

<sup>3</sup>*Instituto de Física, Universidade de Sao Paulo, Caixa Postal 66318, 05315-970 Sao Paulo, SP, Brazil*

(Received 17 October 2005; published 8 May 2006)

We analyze in which experimental conditions the concept of electrical impedance is useful for an electrolytic cell. The analysis is performed by solving numerically the differential equations governing the phenomenon of the redistribution of the ions in the presence of an external electric field and comparing the results with the ones obtained by solving the linear approximation of these equations. The control parameter in our study is the amplitude of the applied voltage, assumed a simple harmonic function of the time. We show that the bulk distribution of ions close to the electrodes differs from the one obtained by means of the linear analysis already for small amplitudes of the applied voltage. Nevertheless, the concept of electrical impedance remains valid. For larger amplitudes, the current in the circuit is no longer harmonic at the same frequency of the applied voltage. Therefore the concept of electrical impedance is no longer meaningful.

DOI: [10.1103/PhysRevE.73.051202](https://doi.org/10.1103/PhysRevE.73.051202)

PACS number(s): 66.10.Ed

### I. INTRODUCTION

The impedance spectroscopy technique is a powerful method for characterizing several electrical properties of media [1]. According to this technique, a sample of the material to be characterized is submitted to an external electrical voltage of amplitude  $V_0$  and frequency  $f = \omega/(2\pi)$  and the electrical current in the external circuit,  $I$ , is measured. By assuming that the system is linear, the current  $I$  is harmonic as the applied voltage and the amplitude of the current is proportional to  $V_0$  [2,3]. In this framework, the electrical impedance  $\mathcal{Z}$ , defined as the applied voltage divided by the current, is independent of the amplitude of the applied voltage. From the analysis of the frequency dependence of  $\mathcal{Z}$  it is possible to deduce the equivalent dielectric constant and equivalent conductivity [4], or the real and imaginary parts of the complex dielectric constant [5], of the sample under consideration. These quantities are not molecular properties of the material to be investigated, but depend, usually, on the thickness of the sample. The true phenomenological parameters characterizing the medium from the dielectric point of view are then derived by means of a theoretical model [6].

The impedance spectroscopy technique is based on the fundamental assumption that the system behaves as a linear system [7]. Only in this case the concept of electrical impedance can be defined. When the system behaves nonlinearly, even if the applied voltage is harmonic, the electrical current in the circuit contains all the harmonics of higher order. The presence of second- and third-order harmonics is responsible for a deviation from the ellipsoidal shape of the parametric curve representing the current versus the applied voltage. Consequently, the electrical impedance depends on the amplitude of the applied voltage and on the time. In this case, in

our opinion, it is no longer possible to derive the dielectric properties of the medium from the analysis of the electrical impedance only.

Our aim is to investigate under which conditions the concept of electrical impedance can be useful from an experimental point of view. In our analysis we consider the case of an electrolytic cell [8]. In this case the fundamental equations describing the redistribution of the ions in the presence of an external electric field are the continuity and drift-diffusion equations for the ions and the Poisson equation for the actual electrical potential [9]. These equations are presented in Sec. II in their general form. The case in which the fundamental equations of the problem can be linearized is also discussed and the concept of electrical impedance introduced. In Sec. III, we compare the numerical solutions for the bulk densities of the ions and for the electric potential across the sample with the solutions obtained by means of the linearized equations. As expected, the two are in good agreement when the amplitude of the applied voltage is small with respect to the thermal voltage—i.e., of the order of 25 mV for monovalent ions at room temperature. Increasing the amplitude of the applied voltage, the agreement is poorer and poorer.

Nevertheless, the concept of electrical impedance remains valid for larger amplitudes. According to our analysis this is due to the fact that the actual bulk density of ions, for intermediate values of the applied voltage, is strongly perturbed only in two surface layers of thickness comparable with the Debye length. Since this length, for the usual materials, is in the submicron scale, the nonlinearity gives a contribution to the impedance variation of the order of Debye length divided by and thickness of the sample, hence negligible. Increasing further the amplitude of the applied potential, the linear approximation fails in the determination of the current in the circuit; hence, we doubt the meaning of the electrical impedance, even though in the literature it is often defined up to quite large values of the applied potential [10–12].

Finally, in Sec. IV we define a certain number of quantities to discuss the deviation of the solution from the linear

\*Electronic address: fernando.freire@polito.it

†Electronic address: giovanni.barbero@polito.it

‡Electronic address: marco.scalerandi@infm.polito.it

approximation. Also, we introduce the concept of a “generalized” impedance, which corresponds to the electrical impedance in the small-amplitude (linear) limit, and we estimate its behavior as a function of the control parameter (applied voltage). We show that the concept of electrical impedance remains good for amplitudes of the applied voltage well beyond the one for which it is reasonable the agreement of the bulk density of ions determined numerically and by means of the linearized equations.

## II. THEORETICAL FRAMEWORK

### A. General equations

Let us consider a cell in the shape of a slab of thickness  $d$  filled with an electrolyte. We suppose that in thermodynamical equilibrium the density of dissociated ions is  $N$  and that dissociation and recombination are negligible. The ions are assumed to be identical in all aspects, except for the sign of the electrical charge  $q$ . We assume the same adsorption energy for positive and negative ions [13,14] and consider perfectly blocking electrodes. In this framework, in the absence of an external electric field, the liquid is locally neutral. When an external electric field is applied, the ions are redistributed close to the electrodes. The liquid is still globally neutral, but locally charged. For the description of our system we use a Cartesian reference frame having the  $z$  axis perpendicular to the limiting surfaces, located at  $z = \pm d/2$ .

We indicate by (i)  $n_p(z, t)$  and  $n_m(z, t)$  the actual density of positive and negative ions, respectively; (ii)  $D$  the diffusion coefficient of the ions in the host liquid; (iii)  $K_B T$  the thermal energy of the ions when the temperature is  $T$ ; (iv)  $V(z, t)$  the actual electrical potential across the sample.

In the presence of an external field the ions move in the sample. The current density is given by

$$j_r = -D \left( \frac{\partial n_r}{\partial z} \pm \frac{q}{K_B T} n_r \frac{\partial V}{\partial z} \right), \quad (1)$$

where  $r = p, m$ . In Eq. (1) there is the sign  $+$  for  $r = p$  and  $-$  for  $r = m$ . The mobility of the ions is defined as  $\mu = Dq/K_B T$ . The differential equations governing the evolution of the bulk densities of ions and of the electrical potential are the conservation law for the number of ions,

$$\frac{\partial n_r}{\partial t} = D \frac{\partial}{\partial z} \left( \frac{\partial n_r}{\partial z} \pm \frac{q}{K_B T} n_r \frac{\partial V}{\partial z} \right), \quad (2)$$

and the Poisson equation [3,15,16]

$$\frac{\partial^2 V}{\partial z^2} = -\frac{q}{\varepsilon} (n_p - n_m). \quad (3)$$

In Eq. (3),  $\varepsilon$  is the dielectric constant of the pure liquid. We have indeed assumed that there is not adsorption from the surfaces; i.e., the ions remain always in the bulk [17].

We write the actual density of ions,  $n_r$ , in the form  $n_r = N + \delta n_r$ . Since  $N$  is the bulk density of ions in the absence of external potential,  $\delta n_r$  represents the perturbation of the density due to the external electric field. In terms of  $\delta n_r$ , Eqs. (2) and (3) become

$$\frac{\partial(\delta n_r)}{\partial t} = D \frac{\partial}{\partial z} \left\{ \frac{\partial(\delta n_r)}{\partial z} \pm \frac{q}{K_B T} (N + \delta n_r) \frac{\partial V}{\partial z} \right\},$$

$$\frac{\partial^2 V}{\partial z^2} = -\frac{q}{\varepsilon} (\delta n_p - \delta n_m), \quad (4)$$

where  $\delta n_r = \delta n_r(z, t)$  and  $V = V(z, t)$ .

We consider a voltage applied to the cell in the form of a harmonic function of amplitude  $V_0$  and frequency  $f = \omega/(2\pi)$ :  $\Delta V(t) = V(d/2, t) - V(-d/2, t) = V_0 \exp(i\omega t)$ . Equations (4) have then to be solved with the boundary conditions

$$\delta n_p(z, 0) = \delta n_m(z, 0) = 0,$$

$$\frac{\partial(\delta n_r)}{\partial z} \pm \frac{q}{K_B T} (N + \delta n_r) \frac{\partial V}{\partial z} = 0,$$

$$V(\pm d/2, t) = \pm (V_0/2) \exp(i\omega t). \quad (5)$$

The first boundary condition implies the equilibrium of the cell before the application of the external electric field, and the second describes perfectly blocking electrodes; i.e., the current densities vanish for  $z = \pm d/2$ . The third boundary condition follows from the assumption that the external power supply is connected so that the electrodes have opposite electric potential.

The system of equations (4) and (5) is nonlinear for the presence of the term  $(N + \delta n_r)(\partial V/\partial z)$  in the equations of continuity. Consequently, even if the applied electrical voltage is harmonic,  $\delta n_r(z, t)$  and  $V(z, t)$  contain all higher-order harmonics.

### B. Linear analysis

A weak external electric field produces only a weak perturbation of the bulk densities of ions—i.e.,  $\delta n_r \ll N$ . In this case it is possible to linearize Eqs. (4) and (5) and the bulk differential equations and boundary conditions become

$$\frac{\partial(\delta n_r)}{\partial t} = D \frac{\partial}{\partial z} \left\{ \frac{\partial(\delta n_r)}{\partial z} \pm \frac{qN}{K_B T} \frac{\partial V}{\partial z} \right\},$$

$$\frac{\partial^2 V}{\partial z^2} = -\frac{q}{\varepsilon} (\delta n_p - \delta n_m), \quad (6)$$

and

$$\frac{\partial(\delta n_r)}{\partial z} \pm \frac{qN}{K_B T} \frac{\partial V}{\partial z} = 0, \quad \text{for } z = \pm d/2,$$

$$V(\pm d/2, t) = (V_0/2) \exp(i\omega t), \quad (7)$$

respectively. Equations (6) and (7) are now linear. Consequently, if the applied voltage is harmonic,  $\delta n_r(z, t)$  and  $V(z, t)$  are harmonic too. In this case, as it has been shown in [18],  $\delta n_r(z, t)$  and  $V(z, t)$  are given by

$$\delta n_r(z, t) = \eta_r(z) \exp(i\omega t),$$

$$V(z,t) = \phi(z) \exp(i\omega t), \quad (8)$$

where

$$\eta_r(z) = \pm p_0 \sinh(\beta z),$$

$$\phi(z) = -2 \frac{q}{\varepsilon \beta^2} p_0 \sinh(\beta z) + cz, \quad (9)$$

with + for  $r=p$  and - for  $r=m$ . The constants  $p_0$  and  $c$  appearing in Eqs. (9) are given by [18]

$$p_0 = - \frac{Nq\beta}{2K_B T (1/\lambda^2 \beta) \sinh(\beta d/2) + i(\omega d/2D) \cosh(\beta d/2)} V_0,$$

$$c = i \frac{\omega}{D} \frac{\cosh(\beta d/2)}{(1/\lambda^2 \beta) \sinh(\beta d/2) + i(\omega d/2D) \cosh(\beta d/2)} V_0, \quad (10)$$

where  $\lambda = \sqrt{\varepsilon K_B T / (2Nq^2)}$  is the Debye length [15] and

$$\beta = \frac{1}{\lambda} \sqrt{1 + i \frac{\omega}{\chi} \lambda^2}. \quad (11)$$

The electric field is given by  $E = -\partial V / \partial z$ . It follows that  $E(z,t) = -\phi'(z) \exp(i\omega t)$ , where the prime means derivation with respect to  $z$ . In particular, the surface electric field is  $E(d/2,t) = -\phi'(d/2) \exp(i\omega t)$ . By means of the Gauss theorem, the surface density of charge sent by the power supply on the electrode can be calculated as  $\Sigma(t) = -\varepsilon E(d/2,t)$ . The total surface electric charge is  $Q = \Sigma S$ , where  $S$  is the surface area of the electrodes. The complex electrical current in the external circuit is  $I = dQ/dt$ . Using the results reported above we obtain

$$I(t) = i\omega \varepsilon S \left\{ -2 \frac{q}{\varepsilon \beta} p_0 \cosh(\beta d/2) + c \right\} \exp(i\omega t). \quad (12)$$

The electrical impedance of the cell, defined as  $\mathcal{Z} = \Delta V(t) / I(t)$ , is

$$\mathcal{Z} = -i \frac{2}{\omega \varepsilon \beta^2 S} \left\{ \frac{1}{\lambda^2 \beta} \tanh(\beta d/2) + i \frac{\omega d}{2D} \right\}. \quad (13)$$

The linear analysis presented above is valid as far as  $|\delta n_r(z,t)| \ll N$ , because only in this case  $n_r(z,t) = N + \delta n_r(z,t)$  can be approximated by  $N$ , as stated above. By taking into account Eqs. (8)–(10) the condition  $|\delta n_r(z,t)| \ll N$  is equivalent to

$$V_0 \ll U = V_T \left| \frac{1}{\lambda^2 \beta^2} + i \frac{\omega d}{2D\beta} \coth\left(\frac{\beta d}{2}\right) \right|, \quad (14)$$

where  $V_T = K_B T / q$  is the thermal voltage of the order of 25 mV for monovalent ions at room temperature.

We conclude that the linearized solution of the equation governing the phenomenon of the ions redistribution in the presence of an electric field holds only if the amplitude is negligible with respect to the amplitude  $U$  defined by Eq. (14). From this equation it follows that in the limit  $\omega \rightarrow 0$ ,  $U \rightarrow V_T$ , as expected [1]. In the opposite limit where  $\omega \rightarrow \infty$ ,  $U$  diverges as  $\sqrt{\omega}$ . This divergence is not surprising. In fact,

for large  $\omega$  the ions cannot follow the rapid variations of the applied voltage and the medium behaves as a true dielectric material.

The existence of an intrinsic voltage  $U$  in the problem is important from a basic point of view, as it has been recently discussed in different situations [19]. However, from a practical point of view, it is fundamental to know when  $U$  is relevant for the determination of the error performed in the measurements of impedance spectroscopy. In particular, it is relevant to determine when it is no longer possible to linearize the equations of the problem, with the resulting dependence of the electrical impedance on the amplitude of the applied voltage and on the time.

### C. Numerical solution

As an alternative to the linearized solution presented in the previous subsection, the complete set of nonlinear equations can be solved numerically. Here, we use, as reported elsewhere [9], a finite-difference (FD) approach [20–22]. We have adopted the usual discretization of both time and space and applied an explicit forward scheme to define both space and time derivatives. The boundary conditions have been implemented as usually performed in diffusion problems [23].

The convergence [21,24] of the proposed scheme has been verified by comparing the numerical solution with the linear approximation at the lower amplitude of the applied voltage. Furthermore, to test convergence also at larger driving amplitudes, we have verified that the solution is not dependent on the steps chosen for both space and time discretization. Finally, the conservation of the total number of ions has been checked at each step of the simulations. As a result of the convergence tests, simulations have been performed using a space step of  $0.0625 \mu\text{m}$ . The time step has been chosen differently for the various frequencies and always smaller than 0.05 ms. Each period of the applied forcing has to be described by a sufficient number of points (at least 500 here) [25].

### III. DEVIATIONS FROM THE LINEAR REGIME FOR INCREASING APPLIED VOLTAGES

The concept of electrical impedance, as defined in Sec. II B, is meaningful only for a linear system. It is then important to define under which conditions the linear approximation of the evolution equations is a reasonable assumption. In particular, here we are interested in analyzing the role of the control parameter, which has been chosen to be the amplitude of the applied potential  $V_0$ . To this purpose, in this section we present a comparison of the numerical results with that obtained from the analytical solution for the linearized case.

For the analysis, we have considered parameters typical of a commercial liquid crystal: monovalent ions ( $q = 1.6 \times 10^{-19}$  A s),  $N = 4.2 \times 10^{20} \text{ m}^{-3}$ ,  $T = 300$  K,  $\varepsilon = 6.7\varepsilon_0$ ,  $D = 8.2 \times 10^{-12} \text{ m}^2/\text{s}$ ,  $d = 25 \mu\text{m}$ , and  $S = 2 \times 10^{-4} \text{ m}^2$  [26]. With these parameters, the Debye length is  $\lambda \sim 0.1 \mu\text{m}$ . Furthermore,  $V_0$  is chosen in the range from 0.1 mV to 5 V, to

A. Results

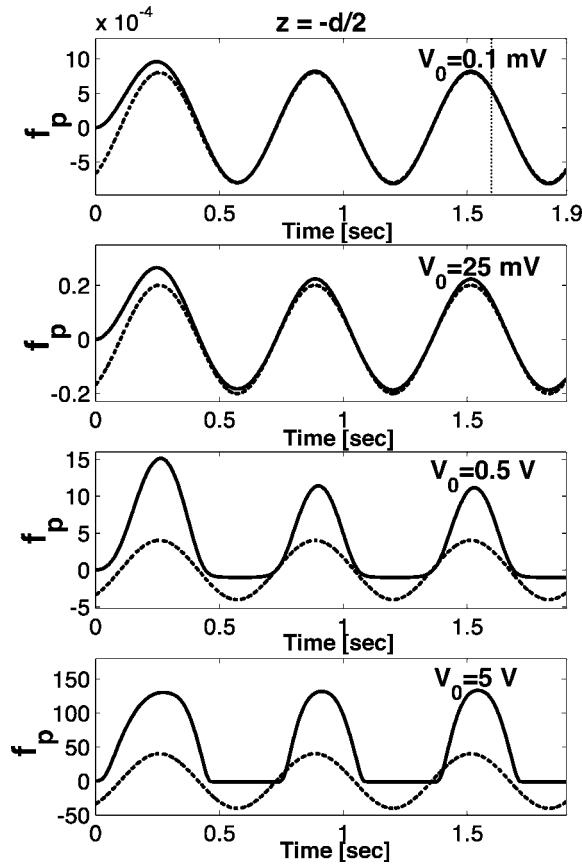


FIG. 1. Temporal evolution of the positive-ion density close to the electrode surface for different values of the applied potential. The numerical solution (solid line) is compared with the linear approximation (dotted line).

cover the wide excursion usually reported in experiments both for low and high voltages [10–12]. Angular frequency is fixed to  $\omega=10$  rad/s. In the next section, under the same experimental conditions, frequency will be varied.

In Figs. 1 and 2, we compare the numerical solution for the positive-ion distribution with the one obtained from the linear analysis. To this purpose we introduce the function  $f_p(z, t) = \delta n_p(z, t) / N = n_p(z, t) / N - 1$ —i.e., the unbalance in the ions distribution. First, in Fig. 1 we plot  $f_p(z=-d/2, t)$ —i.e., the temporal evolution for a point close to the electrode. In the four plots it is clear how the numerical solution (solid line), after a brief transient, reaches very rapidly a stationary condition. Therefore, after one cycle, it is already possible to compare it with the linearized solution (dotted line) which does not describe transient conditions. As expected, the agreement is very good for  $V_0=0.1$  mV, but differences already appear at 25 mV. Note that here  $\delta n_p$  is about 20% of  $N$ —i.e., already relatively large for justifying the linear approximation. For larger amplitudes the two solutions rapidly diverge. The rectification effect, an indication of the presence of higher-order harmonics, is absolutely lost in the linearized solution, which, indeed, predicts unphysical negative values for  $n_p$ . It is interesting to observe the delay of the numerical solution at 5 V.

The profiles  $f_p(z, t=t_0)$  at fixed time are analyzed in Fig. 2 for  $t_0=1.6$  s and  $t_0=1.9$  s—i.e., close to one maximum and one minimum, respectively, of the number of ions close to the electrodes (see Fig. 1). The distribution of ions is perturbed only up to a distance comparable with the Debye length ( $0.1 \mu\text{m}$ ). In this region, the numerical and linearized solutions rapidly diverge with increasing applied potential. Note that the distribution of ions in the bulk is, at any time, almost not modified by the presence of the external field (except that at 5 V). Hence the agreement between the two solutions is always very good (not reported for brevity).

Similar is the agreement found when analyzing the potential. Both the temporal evolution (Fig. 3) close to the center  $V(z=-d/10, t)$  and the profile (Fig. 4) at selected times  $V(z, t=t_0)$  indicate the validity of the linearization procedure for small amplitudes of the applied potential. In both Figs. 3

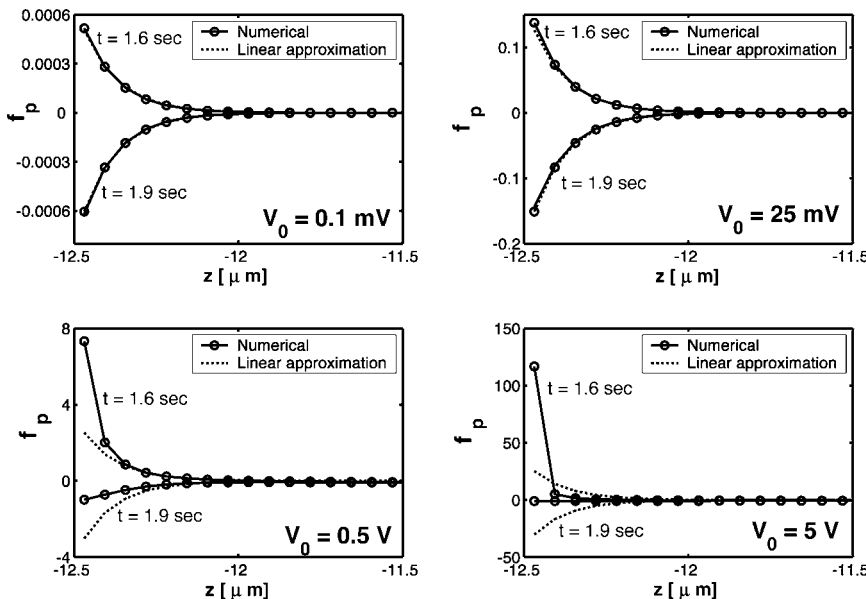


FIG. 2. Profile close to the electrode surface of the positive-ion distribution at different times for different values of the applied potential. The numerical solution (solid line) is compared with the linear approximation (dotted line).

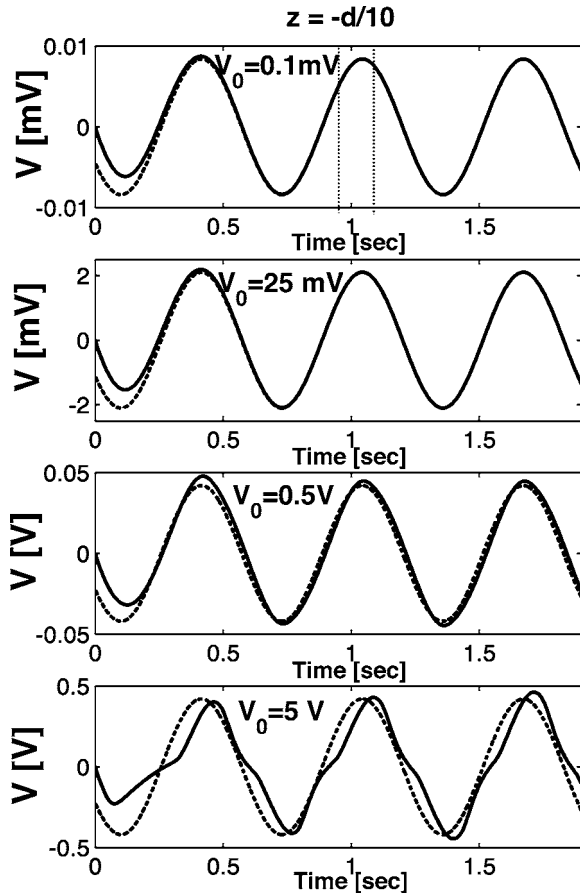


FIG. 3. Temporal evolution of the actual potential in a point close to the center of the specimen for different values of the applied potential. The numerical solution (solid line) is compared with the linear approximation (dotted line).

and 4, distortions at 5 V are particularly evident. A shift similar to the one observed in Fig. 1 is again visible. The analysis of such a shift and the approximately  $\pi/2$  delay between  $f_p$  and  $V$  will be discussed elsewhere [27].

Finally, in Fig. 5 we report the current  $I$  in the circuit as a function of time (first column) and the parametric represen-

tation in the plane  $(\Delta V(t)/V_0, I(t)/I_0)$ , where  $\Delta V(t) = V_0 \sin(\omega t)$  is the applied potential and  $I_0$  corresponds to the maximum of  $I(t)$  (real part of the current). In the linear limit  $I(t) = I_0 \sin(\omega t - \delta)$ ; it follows the parametric representation of an ellipse:  $x = \Delta V(t)/V_0 = \sin(\omega t)$ ,  $y = I(t)/I_0 = \sin(\omega t - \delta)$  rotated of  $45^\circ$  with respect to the Cartesian axes and independent from the applied potential. Any deviation is then a good indication of the nonlinearity of the system.

In the first column of Fig. 5 we can observe again the deviation of the numerical solution from the linear approximation with increasing the applied voltage. Even more significant is the deviation of the solution from the elliptical form, as reported in the right column of Fig. 5. Perfect agreement is found up to 25 mV. For larger  $V_0$ , first the shape remains an ellipse, with only slight distortions (0.5 V). For large voltages (5 V), higher-order harmonics are relevant in the solution and more complicated Lissajou figures start appearing.

**B. Discussion**

Nonlinear effects are always present in the system, and their contributions to the solution increase continuously with increasing  $V_0$ . The linear analysis reported in Sec. II B suggests that the linearization of the system is valid as far as  $\delta n_p \ll N$ —i.e., for applied potentials close to the thermal range (25 mV). The results reported here seem to confirm only partly such an analysis. Indeed, for local variables, such as the density of positive ions, the first distortions appear at  $V_0 = 25$  mV, albeit still small, when  $\delta n_p$  is already quite large (see Fig. 1).

Quite surprisingly, the linear approximation is more robust for global variables, such as the current  $I$  (see Fig. 5). Here, linearization remains valid up to 0.5 V, where  $\delta n_p \sim 15N$ . Nevertheless, as we have shown, in the range  $50 \text{ mV} < V_0 < 1 \text{ V}$  (for the chosen frequency), the presence of the external voltage perturbs considerably the ion distribution only close to the electrodes—i.e. on a surface layer of thickness of the order of a few Debye lengths. The linear approximation for the ion distribution still works very well in

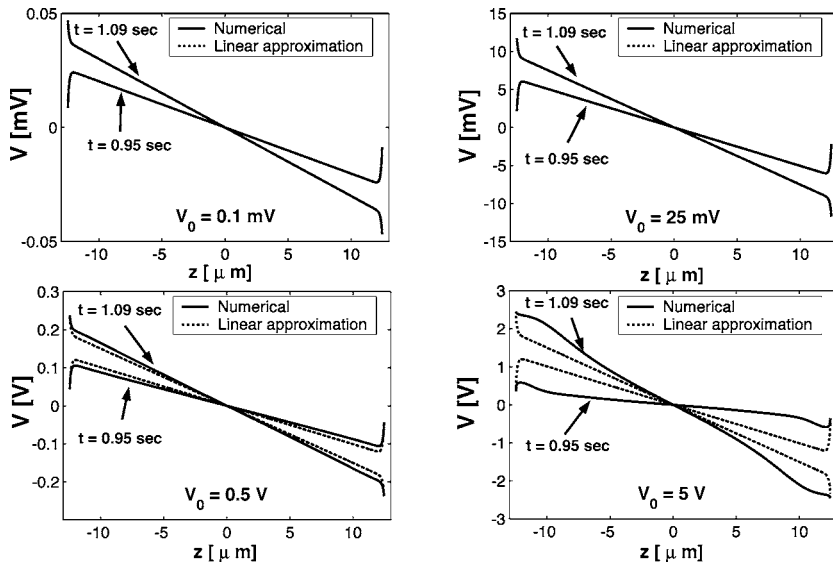


FIG. 4. Profile along the specimen of the actual potential at different times for different values of the applied potential. The numerical solution (solid line) is compared with the linear approximation (dotted line).

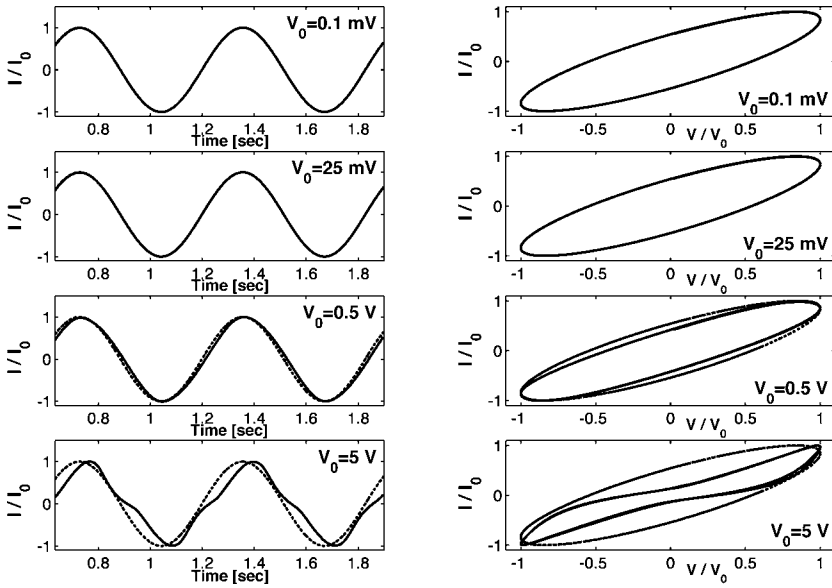


FIG. 5. Comparison of the numerical solution (solid line) with the one obtained from a linear approximation of the model equations (dotted line). Left column: temporal evolution of the electrical current for different values of the applied potential. Right column: parametric representation of the normalized current vs the normalized applied potential. Deviations from the ellipse indicate the presence of high nonlinear effects.

the bulk of the material. As a consequence, the effects on the electrical current is of the order of the ratio between the Debye length and the layer thickness—i.e., very small. It follows that the electrical current remains harmonic as in the linear case.

Increasing further the applied voltage—e.g., larger than 1 V, the distribution of ions is perturbed in all the sample. Consequently deviations from the linear solution appear also for the electrical current (see, e.g., results at 5 V).

#### IV. ANALYSIS OF THE CONCEPT OF ELECTRIC IMPEDANCE

##### A. Quantifiers

The results reported in the previous section indicate that the system behaves “reasonably” linearly only up to some applied voltage. Nevertheless, they do not allow us to define

this “threshold” voltage  $V_C$ , nor to analyze its dependence on parameters, such as the frequency of the applied voltage.

In Fig. 6 we show again the parametric curve  $(x,y) = (\Delta V(t)/V_0, I(t)/I_0)$ , as in the second column of Fig. 5. The applied potential is fixed ( $V_0 = 0.5$  V), and the distortion from the elliptical shape is analyzed for different frequencies. The linear approximation (dots) always predicts an ellipse rotated of  $45^\circ$  with respect to the axes and width decreasing with increasing frequency in the range 0–100 rad/s. The numerical solution deviates considerably from the linearized one, with distortions decreasing with increasing frequency and completely disappearing at  $\omega = 100$  rad/s. This constitutes a preliminary indication that the threshold potential moves to larger values for higher frequencies, as expected.

The results reported in Fig. 6 suggest that the critical frequency below which nonlinearities due to ionic motion set in is rather small. This is to be expected. In fact, in a recent

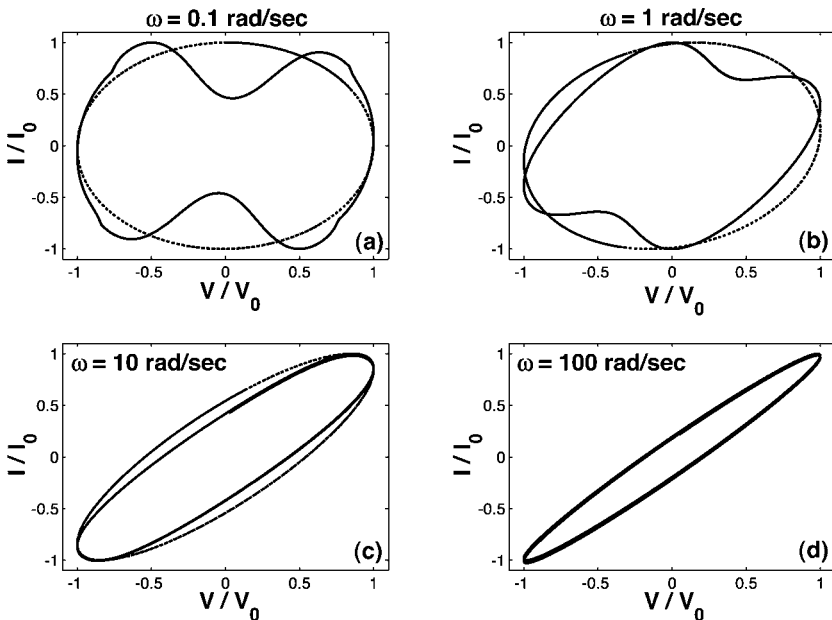


FIG. 6. Parametric representation of the normalized current  $I(t)/I_0$  vs the normalized applied potential  $V(t)/V_0$  for different values of frequency and  $V_0 = 0.5$  V. Deviations from the ellipse indicate the presence of high nonlinear effects.

investigation we have analyzed transient effects in an electrolytic cell submitted to a step like external voltage in order to determine the relaxation time of the redistribution of the ions and of the potential [28]. The analysis showed that, in the limit of external potentials up to 1 V, the relaxation time is given by  $\tau_r = \lambda d / 2D$ . It follows that we can consider a relaxation frequency  $\omega_r = 2\pi / \tau_r$ , which for our choice of parameters is of the order of 40 Hz. In the case considered here (sinusoidal forcing), we can therefore expect that ions do not participate in the dynamics of the system (i.e., absence of nonlinear effects) as long as  $\omega > \omega_r$ . In fact, for large frequencies, the ions response is not fast enough to respond to the applied field and the system behaves like a pure capacitor.

To quantify the effect, two quantifiers may be introduced.

(i) An indicator for the ions distribution:

$$\Delta_p(z, V_0) = \frac{1}{T} \int_t^{t+T} [f_p(z, t'; V_0) - f_p^{lin}(z, t'; V_0)]^2 dt', \quad (15)$$

where  $T = 2\pi / \omega$  is the period and the superscript *lin* indicates the solution deduced in the linearized case. The amplitude of the applied voltage has been explicitly indicated as a control variable in  $f_p$ . Considering that the maximum of the deviations are closer to the electrodes, in the following we will consider  $z = -d/2$ .

(ii) An indicator for the electrical current:

$$\Delta_I(V_0) = \frac{1}{T} \int_t^{t+T} \left[ \frac{I(t'; V_0)}{I_0} - \frac{I^{lin}(t'; V_0)}{I_0^{lin}} \right]^2 dt'. \quad (16)$$

This quantity provides an indication of the distortion from the expected ellipsoidal shape in the parametric representation described before.

The behavior of the two indicators is reported in Figs. 7(a) and 7(b), respectively, for different frequencies of the applied potential. Both figures indicate, as expected, an increase in the deviation from the linear solution with increasing amplitude. In both cases, the contribution of the nonlinear terms is smaller for larger frequencies (at any given amplitude), as already remarked before.

Figure 7(a) shows a power-law dependence  $\Delta_p = a_1 V_0^{a_2}$ . The coefficient  $a_1$  decreases with increasing  $\omega$ , while the exponent is frequency independent. Note that a value of the indicator of 0.1 (i.e., a discrepancy of 3% between the numerical solution and the linear approximation) corresponds to applied voltages ranging from 10 mV to 100 mV, depending on the frequency. The results show also a small dependence from frequency at low values of  $\omega$ , in agreement with previous observations [29].

Deviations from the linear solution increase less rapidly for the second quantifier  $\Delta_I$ , reported in Fig. 7(b). Here it is interesting to note that, albeit  $\Delta_I$  increases with continuity as a function of  $V_0$ , a threshold voltage is evident, located at about 50 mV for the smaller frequencies and about 0.8 V for the higher frequency. This constitutes an indication of the possibility to individuate a parameter for discriminating between the linear and nonlinear behaviors of the system, at least for what concerns its global variables, such as the current  $I$ .

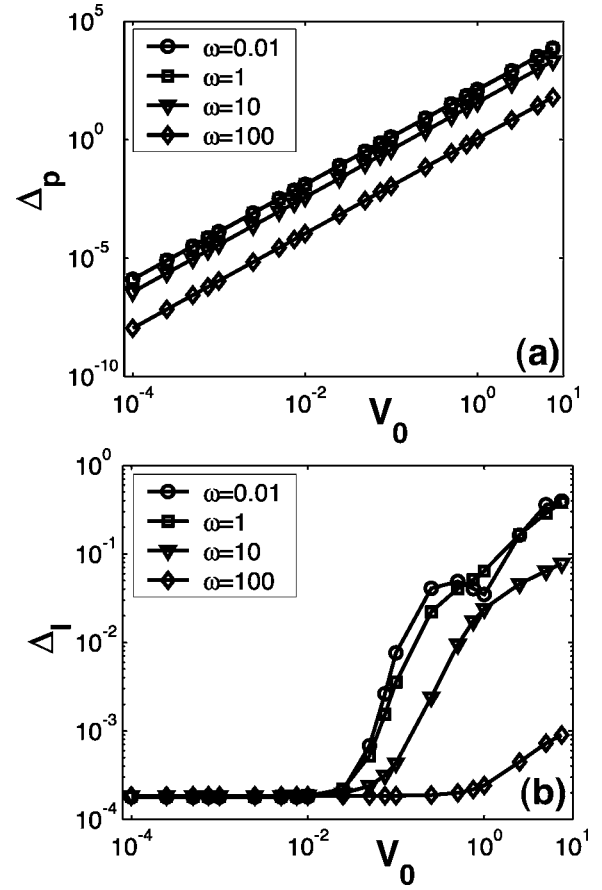


FIG. 7. (a) Quantifier for the deviation in the number of ions  $\Delta_p$  [see Eq. (15)] vs the amplitude  $V_0$  of the applied voltage for different values of frequency. (b) Quantifier for the deviation in the current  $\Delta_I$  [see Eq. (16)] vs the amplitude  $V_0$  of the applied voltage for different values of frequency.

## B. Generalized impedance

The quantifiers introduced in the previous subsection still have the disadvantage of not being directly related to experimentally detected quantities and variables. More meaningful is to introduce some quantity directly related to the electric impedance of the cell. As already remarked, the impedance is in general defined from the relation between applied potential and the response of the system in terms of electric current:  $Z = \Delta V / I$ . As such the impedance is a complex quantity and, in the linear approximation, its modulus is  $Z = |Z| = V_0 / I_0$ .

Unfortunately, when the system is nonlinear, the definition given for the impedance is no longer meaningful. In fact, whenever distortions from the linear case appear,  $Z$  becomes time and amplitude dependent. For this reason, we propose here the introduction of a generalized electrical impedance  $Z_G$  which, in the limit of vanishing applied potential, converges to the value defined in the linear analysis. To this purpose, we introduce the function

$$\xi(t; V_0) = 2 \frac{I^2(t; V_0)}{V_0^2}. \quad (17)$$

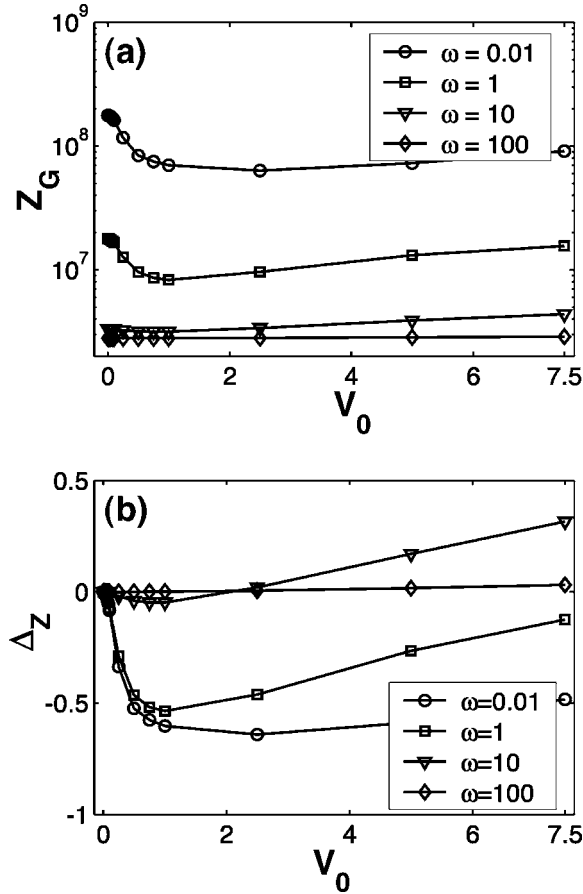


FIG. 8. Dependence of the generalized electrical impedance  $Z_G$  [see Eq. (20)] on the amplitude of the applied potential. (a) Numerical results for the value of  $Z_G$ . The linear approximation predicts a constant value for the electric impedance, equal to the value assumed by  $Z_G$  when  $V_0 \rightarrow 0$ . (b) Deviation  $\Delta_Z$  of the calculated  $Z_G$  from its linear approximation [see Eq. (21)] for different frequencies.

In the linear case (in which  $V_0 \rightarrow 0$ ), the average value of  $\xi$  gives the square of the modulus of the electric admittance:  $Y = 1/|Z|$ . In fact, a simple calculation gives

$$\langle \xi(t;0) \rangle = \frac{1}{T} \int_t^{t+T} \xi(t';0) dt' = Y^2(0). \quad (18)$$

In the general case we can define a generalized admittance  $Y(V_0)$  which is dependent on the applied voltage amplitude:

$$Y^2(V_0) = \langle \xi(t;V_0) \rangle = \frac{1}{T} \int_t^{t+T} \xi(t';V_0) dt'. \quad (19)$$

We then have a definition of a generalized electrical impedance:

$$Z_G(V_0) = 1/Y(V_0). \quad (20)$$

It follows that the quantity

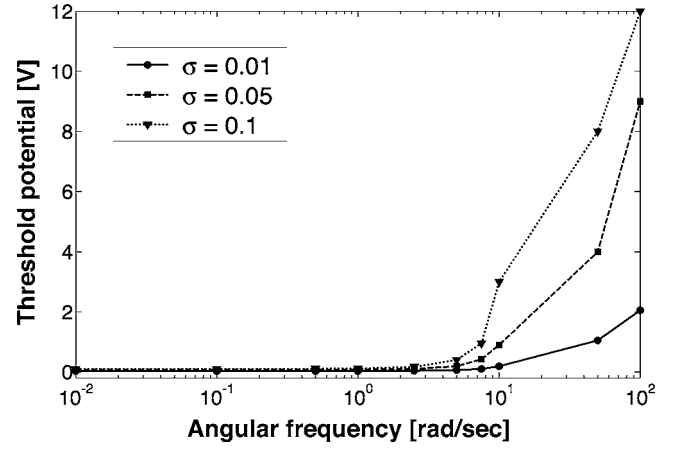


FIG. 9. Threshold potential for the validity of the linear approximation as a function of frequency. The linear approximation is valid only for potentials lower than the threshold—i.e., in the region below the curve. The three curves refer to different choices of the error tolerance  $\sigma$  for the electrical impedance. Curves may look very different if the tolerance is defined on other quantities. In particular, the curve flattens down when the error is calculated on the distribution of positive ions, with results similar to that reported in [18].

$$\Delta_Z = \frac{Z_G(V_0) - Z(0)}{Z(0)} \quad (21)$$

provides information about the deviation of the electrical impedance at a given amplitude from the one expected from the linear analysis.

In Fig. 8(a) we report the generalized impedance as a function of the applied voltage for different frequencies. As expected  $Z_G$  converges to  $Z$  for low values of the driving voltage. The generalized impedance, as the linear one, increases with decreasing frequencies. The dependence of  $Z_G$  on  $V_0$  is quite large, confirming the inadequacy of a linear approximation already for low voltages. Also, the dependence is not monotonous. A further analysis of this observation is currently in progress.

$\Delta_Z(V_0)$  vs  $V_0$  is reported in Fig. 8(b). The general behavior shows that the error is negligible for low voltages. Increasing  $V_0$ , the linear analysis first overestimates the actual impedance (negative  $\Delta_Z$ ), with variations up to 50% (for the lowest frequencies). For large voltages, the linear analysis underestimates the impedance of the system. By changing  $\omega$  the curve  $\Delta_Z(V_0)$  vs  $V_0$  does not change its shape, but it is shifted to the right and rescaled, indicating an almost linear behavior up to 7.5 V for  $\omega = 100$  rad/s.

Finally, in Fig. 9 we define a threshold voltage  $V_C$ . This quantity is defined as the amplitude of the applied potential at which  $|\Delta_Z|$  is larger than an assigned precision  $\sigma$ , which may be determined, e.g., by the experimental accuracy. We suggest that, given  $\sigma$ , the linear analysis, hence the traditional concept of electrical impedance, is valid only for voltages lower than  $V_C$ . Of course, the threshold voltage depends on frequency and on the precision required, as reported in Fig. 9. The general behavior is in agreement with previously reported predictions, based only on the validity of the linear

approximation  $\delta n \ll N$ ; i.e., the threshold voltage is in the thermal range and independent from frequency for low frequencies, while increases almost exponentially at large frequencies. Nevertheless, we remark here that the absolute values of  $V_C$  are much larger than the ones previously estimated [29]. For instance, a threshold potential was estimated of about 25 mV for low frequencies, while here we have  $V_C(\omega \rightarrow 0) \sim 70$  mV. The discrepancy is even larger at high frequencies. We estimate a threshold potential of the order of 1 V at  $\omega = 50$  rad/s, versus an estimate of 50 mV previously reported. This result is encouraging, suggesting the validity of the linear approximation in a range much larger than previously expected. Nevertheless, it also points out that much carefulness is needed at large voltages than usually adopted.

## V. CONCLUSIONS

We have investigated the redistribution of the ions in an electrolytic cell submitted to an external harmonic electric field. We have solved numerically the fundamental equations of the problem under investigation by considering as electrolyte a commercial nematic liquid crystal. The thickness of the sample has been assumed to be 25  $\mu\text{m}$ , as the ones used in display technology. Following the standard procedure, we have also solved the same equations in the linear approximation, where the presence of the external field produces only a small variation of the bulk density of ions with respect to the one in thermodynamical equilibrium, in the absence of an external field.

By considering the amplitude of the applied voltage as a control parameter, we have compared the numerical solution with the one relevant to the linearized equations. We have analyzed, in particular, the phenomenon in the low-frequency region ( $\omega \leq 100$  rad/s). According to our analysis, in the range in which the amplitude of the applied voltage is of the order of the thermal voltage, the presence of the external voltage perturbs the ions distributions only close to the electrodes on a surface layer whose thickness is comparable with the Debye length. Consequently, the linear approximation works well in the bulk of the sample. In this framework, the concept of electrical impedance is useful and the impedance spectroscopy technique can give useful information on the dielectric properties of the medium. On the contrary, when the amplitude of the applied voltage is of the order of 1 V, the distribution of ions is strongly perturbed in all the sample. In this case, in the low-frequency range, the concept of electrical impedance is meaningless and the measurement by means of impedance spectroscopy methods of the dielectric parameters is questionable. We have also investigated the role of the frequency in the validity of the linear approximation. In this case, we have shown that for  $\omega = 100$  rad/s, the concept of electrical impedance remains valid up to amplitude of the applied voltage of the order of 1 V.

## ACKNOWLEDGMENTS

We thank Professor A. Strigazzi (Politecnico di Torino, Italy) for useful discussions. One of us (F.C.M.F.) acknowledges financial support received from CAPES (Brazil).

- 
- [1] J. Ross Macdonald, *Impedance Spectroscopy* (John Wiley and Sons, New York, 1987), Chap. 1.
  - [2] J. Jamnik and J. Maier, *J. Electrochem. Soc.* **146**, 4183 (1999).
  - [3] P. A. Cirkel, J. P. M. van der Ploeg, and G. J. M. Koper, *Physica A* **235**, 269 (1997).
  - [4] S. Uemura, *J. Polym. Sci., Polym. Phys. Ed.* **10**, 2155 (1972).
  - [5] A. Sawada, Y. Nakazono, K. Tarumi, and S. Naemura, *Mol. Cryst. Liq. Cryst. Sci. Technol., Sect. A* **318**, 2251 (1998).
  - [6] J. R. Macdonald, *Trans. Faraday Soc.* **66**, 943 (1970).
  - [7] J. R. Macdonald, *Electrochim. Acta* **35**, 1483 (1990).
  - [8] A. D. Hollingsworth and D. A. Saville, *J. Colloid Interface Sci.* **257**, 65 (2003).
  - [9] M. Scalerandi, P. Pagliusi, G. Cipparrone, and G. Barbero, *Phys. Rev. E* **69**, 051708 (2004).
  - [10] A. Sawada, K. Tarumi, and S. Naemura, *Jpn. J. Appl. Phys., Part 1* **38**, 1418 (1999).
  - [11] S. Murakami and H. Naito, *Jpn. J. Appl. Phys., Part 1* **36**, 773 (1997).
  - [12] S. Murakami, H. Iga, and H. Naito, *J. Appl. Phys.* **80**, 6396 (1996).
  - [13] M. Scott, R. Paul, and K. V. I. S. Kalert, *J. Colloid Interface Sci.* **230**, 377 (2000).
  - [14] M. Scott, R. Paul, and K. V. I. S. Kalert, *J. Colloid Interface Sci.* **230**, 388 (2000).
  - [15] J. Israelachvili, *Intermolecular Forces* (Academic Press, London, 1985), Chap. 12.
  - [16] M. Z. Bazant, K. Thornton, and A. Ajdari, *Phys. Rev. E* **70**, 021506 (2004).
  - [17] G. Barbero, *Phys. Rev. E* **71**, 062201 (2005).
  - [18] G. Barbero and A. L. Alexe-Ionescu, *Liq. Cryst.* **32**, 943 (2005).
  - [19] G. Barbero, A. L. Alexe-Ionescu, and I. Lelidis, *J. Appl. Phys.* **98**, 113703 (2005).
  - [20] J. Strickwerda, *Finite Difference Schemes and Partial Differential Equations* (Wadsworth-Brooks, London, 1989).
  - [21] A. C. Vliegthart, *J. Eng. Math.* **5**, 137 (1971).
  - [22] M. Scalerandi, A. Romano, and C. A. Condat, *Phys. Rev. E* **58**, 4166 (1998).
  - [23] G. Kaniadakis, P. P. Delsanto, and C. A. Condat, *Math. Comput. Modell.* **17**, 31 (1993).
  - [24] M. Scalerandi, P. P. Delsanto, C. Chiroiu, and V. Chiroiu, *J. Acoust. Soc. Am.* **106**, 2424 (1999).
  - [25] E. Ruffino and P. P. Delsanto, *Comput. Math. Appl.* **38**, 89 (1999).
  - [26] A. Sawada, K. Tarumi, and S. Naemura, *Jpn. J. Appl. Phys., Part 1* **38**, 1423 (1999).
  - [27] G. Barbero, F. C. M. Freire, and M. Scalerandi (unpublished).
  - [28] A. L. Alexe-Ionescu, G. Barbero, F. C. M. Freire, and M. Scalerandi (unpublished).
  - [29] G. Barbero and L. R. Evangelista, *Adsorption Phenomena and Anchoring Energy in Nematic Liquid Crystals* (CRC Press, Boca Raton, 2005).